LunaIcy Mathematical Exploration and Reimplementation

by Arne Huckemann
arne.jean-cedric.huckemann@students.uni-mannheim.de

CONTENTS

Contents **1**

1 LunaIcy Mathematical Exploration **2**

1 Physics behind the model . . . 5
1.1 Physics behind the ODE . . . 5
1.2 Physics behind the PDE . . . 5
2 Numerical Solution of the ODE . . . 6
3 Numerical Solution of the PDE . . . 7
4 Geometry . . . 9
4.1 Grain Volume . . . 9
4.2 Bond Volume . . . 9
4.3 Surface Area and Curvature . . . 10
4.4 Finding the Intersection of Bond and Grain Area . . . 10

2 Implementation **11**

1 Simulations . . . 11
2 Outlook . . . 12

A Appendix **14**

1 Grain Volume . . . 14

Bibliography **16**

1

LUNAICY MATHEMATICAL EXPLORATION

Abstract

The paper "LunaIcy" [2] models thermally coupled sintering of ice grains and their bonds in the ice sheet of Jupiter's moon Europa. This report attempts to reimpliments this model using modifications. In the paper sintering was modeled via a system of ODEs that where coupled with a non-standard heat equation. In contrast to the paper this report uses the numerical scheme of implicit Euler to solve the ODE and by doing so, avoids the limitation of the small step size that occur due to the stiffness of the problem. Additionally, here, a solver specifically tailored for the non-standard heat equation is proposed. It handles the Neumann boundary data by incorporating ghost cells and solves the PDE with the method of lines. The resulting system of ODEs is, again, due to stiffness, solved via implicit Euler. As in the given PDE there is no standard Laplace operator, a three point stencil cannot be derived using finite differences directly. Using finite volumes combined with finite differences, however, yields a three point method allowing for computational efficiency. The appendix details the derivation of the grain-bond geometry using manifold integrals, offering a generalized framework for future exploration of complex grain shapes.

Motivation: In light of the upcoming missions planned to Jupiter's moon Europa such as JUICE and in particular in view of a mission that might attempt to drill through the ice sheet, the geometry of the ice grains are of great interest. A model trying to predict the microstructure for the ice sheet should not only depend on sintering, but also on external influences such as temperature, radiation and micro meteor impacts. A deterministic model was proposed in "LunaIcy" [2] that couples sintering and temperature. In order for the model to incorporate micro meteor impacts, it could be extended to a stochastic one. In order to make worst case bounds on the microstructure of such a stochastic model one could use extreme value theory for stochastic processes. This is briefly motivated in the outlook. The rest of this report focuses on the reimplementation of the deterministic model.

Consider a one-dimensional slice of the Ice sheet of Jupiter's moon Europa. This gives our state space $\Omega := [0, d] \subset \mathbb{R}$ where d denotes the depth of the ice sheet. We now try to model the changing of ice grains and their bonds to neighboring grains such that a steady state (fixed point of the dynamic system) is reached. This steady state aims to explain the ice grain and bond size in the ice sheet of Europa. In [2] it was proposed that low thermal inertia of porous ice allows us to presume that the depth of significant temperature changes before dissipation is very low (only a few centimeters). The ice sheet can be limited to only a small depth d. Further, due low thermal inertia the bottom boundary data for the yet to be defined heat equation should ensure that the temperature change is zero, when reaching the bottom.

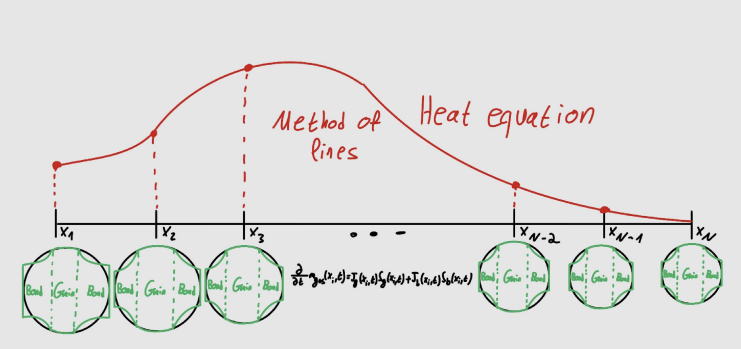

Figure 1.1: Overview of the discretization space Ω_h and the microstructure at each grid point and temperature that is coupled.

Choose some discretization of the state space $\Omega_h \subset \Omega$ where $|\Omega_h|$ is the number of grid points of the slice. Note that every grid point is an average representation of many ice crystals. The one we model via grid point is supposed to be an average representation of these crystals. In every grid point $x \in \Omega_h$ we denote the microstructure by $(r_g(x,t), r_b(x,t))^T$, where r_g is the grain radius and r_b is the bond radius at time $t \geq 0$.

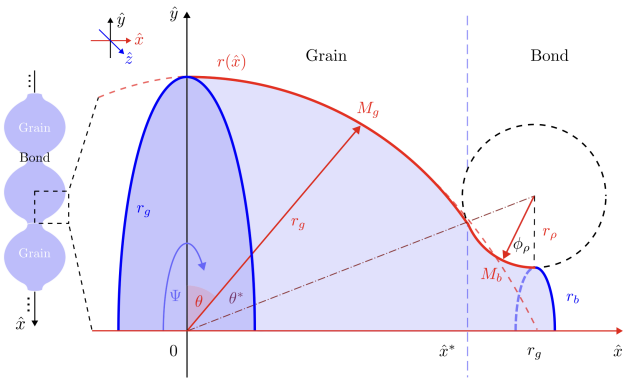

Figure 1.2: Illustration of the grain and bond geometry [2]. In this report I denoted the the surfaces M_g and M_b as S_g and S_b, respectively. They describe the surface area of the grain and bond, respectively.

The change of radii/microstructure is modeled indirectly via the water vapor transport. Consider the conservation law (i.e. assuming a closed system that does not lose or gain mass)

$$\frac{\partial}{\partial t}(m_g(x,t) + m_b(x,t) + m_{gas}(x,t)) = 0, \quad x \in \Omega_h, t \geq 0,$$

where m_g is the mass of the grain, m_b mass of the bonds between two grains (we assume two bonds for each grain) and m_{gas} the mass of the surrounding gas vapor in the pores. Note that this conservation law is assumed to be locally valid, i.e. for every $x \in \Omega_h$, i.e. we do not assume that gas mass moves between grid points. Allowing for mass to move between grid points could be a future extension.
A benefit of the approach of modelling the masses is that we do not make assumptions on the underlying initial water vapor pressure, but only on its initial mass. Using the Hertz-Knudsen formula, mass transport only occurs, proportionally to the difference in gas pressure in the pore space and the saturated water vapor

pressure over a flat surface. It is defined for every $x \in \Omega_h$ as

$$\begin{aligned}&\frac{\partial}{\partial t} m_{gas}(x,t)\\ &= J_g\left(t, T(x,t), r_g(x,t), m_{gas}(x,t)\right) S_g(t, r_g(x,t)) + J_b(t, T(x,t), r_b(x,t), m_{gas}(x,t)) S_b(t, r_g(x,t), r_b(x,t))\\ &=: J_g(x,t) S_g(x,t) + J_b(x,t) S_b(x,t),\end{aligned} \tag{1.1}$$

which is an asymptotic stable linear ODE (in Section 2.1 it can be seen that the fluxes J_g and J_b are linear in m_{gas} and have negative derivatives). Here S_g denotes the surface area of the grain in contact with the outward gas and J_g the respective flux, $S_b(t)$ the surface area of the bond in contact with the gas and again J_b the respective flux. Only if these fluxes are non-zero sublimation will occur. Because this is a linear and asymptotically stable ODE, there exists a global fixed point, which we assume is reached instantaneously, i.e. assume

$$\frac{\partial}{\partial t} m_{gas}(x,t) = 0. \tag{1.2}$$

Then grain/bond gains/losses of mass is described by

$$\frac{\partial}{\partial t} m_i(x,t) = -J_i(x,t) S_i(x,t), \quad i = g, b. \tag{1.3}$$

As we will soon see the heat equation needs the radii r_g, r_b as inputs to calculate the thermal conductivity of bonds and grains. Thus, we need to recover the radii from the masses. This can be done by first calculating the respective volumes:

$$V_g(x,t) = \frac{m_g(x,t)}{\rho_0}, \quad V_b(x,t) = \frac{m_b(x,t)}{\rho_0}, \tag{1.4}$$

where ρ_0 is the bulk Ice density. Then we can retrieve their respective radii via

$$f\big(m_g(x,t), m_b(x,t)\big) := \begin{pmatrix} r_g(x,t) \\ r_b(x,t) \end{pmatrix} = \arg\min_{r_g, r_b} \begin{pmatrix} |\frac{m_g(x,t)}{\rho_0} - v_g(r_g, r_b)| \\ |\frac{m_b(x,t)}{\rho_0} - v_b(r_g, r_b)| \end{pmatrix}, \tag{1.5}$$

where v_g will be calculated using Equation (1.11) and (1.12). As seen in Figure 1.2 at depth $\hat{x}^*$ the two surface areas of grain and bond intersect (actually circle). While optimizing f for r_g and r_b for every radii pair suggested by the minimization problem, $\hat{x}^*$ is calculated in (1.13). This is briefly touched upon in Section 5.4. Solving Equation (1.5) will not further be discussed, as standard optimization suffices.

We have now described the dynamics for each microstructure at a specific grid point $x \in \Omega_h$, i.e. we have a system of $|\Omega_h|$ many ODEs. As seen in the definitions of the fluxes (1.9), they also depend on the local temperature $T(x,t)$, i.e. the temperature of $x \in \Omega_h$ at time $t \geq 0$. This means the system is now coupled with a heat equation on the same grid. The average temperature at $x \in \Omega_h$ is modelled via the heat equation with Neumann boundary data

$$\rho c_p \frac{\partial}{\partial t} T(x,t) = \frac{\partial}{\partial x}\left(k\big(f(m_g(x,t), m_b(x,t))\big) \frac{\partial}{\partial x} T(x,t) \right), \quad x \in \Omega, t > 0 \tag{1.6}$$

$$k(f(m_g(0,t), m_b(0,t))) \frac{\partial}{\partial x} T(0,t) = -F_{solar}(t) + \epsilon \sigma_{SB} T(0,t)^4 \tag{1.7}$$

$$k(f(m_g(d,t), m_b(d,t))) \frac{\partial}{\partial x} T(d,t) = 0, t > 0 \tag{1.8}$$

$$T(x,0) = T_0(x), \quad \forall x \in \Omega,$$

where $\rho, c_p \in \mathbb{R}$ are constants and k denotes the thermal conductivity that couples the ODE to the PDE. For ease of notation we will write $k(x,t) := k(f(m_g(x,t), m_b(x,t)))$. $T_0(x)$ is the initial Temperature at the grid points. Lastly, F_{solar} is the energy that comes from the sun and σ_{SB} and ϵ model how temperature from the surface radiates into the vacuum of space.
Thus, in total we need to solve in each time step for m_{gas}, the ODE in (1.3), the optimization problem in (1.5) and the PDE (1.6).

1 Physics behind the model

Here is a brief physics overview.

1.1 Physics behind the ODE

The pressure of the surrounding gas/water vapor is written as $P_{gas}(x,t)$ at time t and $x \in \Omega_h$. $P_{K_j}(x,t)$ denotes the equilibrium vapor pressure the a curved surface of grain and bond with average curvature K_i, $i = g, b$. Note that in general it holds for equal area:

$$\text{convex surface pressure} > \text{flat surface pressure} > \text{concave surface pressure}.$$

The flux of a grain or a bond is then given by

$$J_i(x,t) := \alpha(P_{K_i}(x,t) - P_{gas}(x,t))\sqrt{\frac{M}{2\pi RT(x,t)}}, \quad i = g, b, \tag{1.9}$$

where $\alpha, R, M \in \mathbb{R}$ are constants and $T(x,t)$ denotes the temperature of the grain at point $x \in [0,d]$ at time $t \geq 0$. Here α is the sticking coefficient, R is the universal molar gas constant and M the molar mass of water. The curved surface pressure is given by

$$P_{K_i}(x,t) := P_{sat}(T(x,t))\left(1 + \frac{\gamma M}{RT(x,t)\rho_0} K_i(f(m_g(x,t), m_b(x,t))^T e_i)\right), \quad i = g, b, \tag{1.10}$$

where $\gamma, \rho_0 \in \mathbb{R}$ are constant, where γ is the water surface tension, ρ_0 the bulk ice density and e_i is the standard unit vector. $P_{sat}(T(x,t)) = P_0 e^{-\frac{Q_{sub}}{RT(x,t)}}$ is the saturated water pressure of a flat surface. Here $P_0, Q_{sub} \in \mathbb{R}$ are constants, where P_0 is called high temperature pressure limit, because theoretically, as the temperature goes to infinity, this saturated water pressure of a flat surface will be equal to $P_0 \cdot 1$. Q_{sub} is the activation energy for sublimation. Further,

$$P_{gas}(T(x,t)) := \frac{m_{gas}(x,t)RT(x,t)}{MV_{pore}} = \frac{(1-\phi)m_{gas}(x,t)RT(x,t)}{MV_g(x,t)\phi}, \quad V_{pore} := V_g(x,t)\frac{\phi}{1-\phi},$$

where $V_g(x,t)$ denotes the volume of the grain (1.4), m_{gas} the equilibrium mass of water vapor mass and ϕ denotes the porosity.

1.2 Physics behind the PDE

The lower boundary data was described in the introduction being set in such a way, that no temperature flows at the bottom. Here we will briefly describe the upper boundary data. Remember from (1.7) that

$$k(0,t)\frac{\partial}{\partial x}T(0,t) = -F_{solar}(t) + \epsilon\sigma_{SB}T(0,t)^4.$$

The function F_{solar} gives us the day and night cycle (eclipses by Jupiter and other moons are omitted) and the term $\epsilon\sigma_{SB}T(0,t)^4$ describes the thermal radiation from the surface into vacuum, where ϵ denotes the emissivity of the ice surface, i.e. the ratio of the total radiant exitance of the material surface to that of an ideal black body at the same thermodynamic temperature. σ_{SB} is the fundamental Stefan-Boltzmann constant. The first summand of (1.7) depends on λ, the latitude of the site in question on Europa and ψ its longitude:

$$F_{solar}(t,\lambda,\psi) := (1-A(\lambda,\psi))\frac{G_{sc}}{d(t)^2}\cos(\theta_i(t,\lambda,\psi))\mathbf{1}_{\{\cos(\theta_i(t,\lambda,\psi))>0\}},$$

where A is the surface albedo, G_{sc} the solar constant and θ_i is the solar incidence angle and $d(t)$ is the distance to the sun. Note that using this indicator function we can easily model day and night cycle.
The other terms in the above heat equation are described as follows.

$$\rho(\phi) = \rho_0(1-\phi)$$

is the density of porous ice and c_p is the ice heat capacity constant. Note that the paper [2] reasons that we can choose these two as constant, as it argues that the sintering process on Europa is primarily driven by evaporation and condensation, i.e. the pores volume is assumed to stay constant. The thermal conductivity is given by

$$k(\phi, r_b, r_g) = \frac{567}{T(x,t)}(1-\phi)\frac{r_b}{r_g}.$$

This last term here links the PDE to the ODE that describes sintering.

2 Numerical Solution of the ODE

First we need to solve for the equilibrium mass of the water vapor mass $m_{gas}(x,t)$ in each state $x \in \Omega_h$ at time $t \geq 0$. Remember the conservation law, which yielded that $\frac{\partial}{\partial t}m_{gas}(x,t) = 0$. We can solve it by an algebraically solvable equation:

$$\begin{aligned}
0 &= \frac{\partial}{\partial t}m_{gas}(x,t) = J_g(x,t)S_g(x,t) + J_b(x,t)S_b(x,t)\\
&= S_g\alpha\sqrt{\frac{M}{2\pi RT(x,t)}}\left(P_{sat}(T(x,t))\left(1+\frac{\gamma M}{RT(x,t)\rho_0}K_g\right) - P_{gas}(T(x,t))\right)\\
&+ S_b\alpha\sqrt{\frac{M}{2\pi RT(x,t)}}\left(P_{sat}(T(x,t))\left(1+\frac{\gamma M}{RT(x,t)\rho_0}K_b\right) - P_{gas}(T(x,t))\right)\\
&= \alpha\sqrt{\frac{M}{2\pi RT(x,t)}}\left((S_g+S_b)P_{sat}(T(x,t)) + S_gP_{sat}(T(x,t))\frac{\gamma M}{RT(x,t)\rho_0}K_g + S_bP_{sat}(T(x,t))\frac{\gamma M}{RT(x,t)\rho_0}K_b\right)\\
&- \alpha\sqrt{\frac{M}{2\pi RT(x,t)}}P_{gas}(T(x,t))(S_g+S_b)\\
&= P_{sat}(T(x,t))\alpha\sqrt{\frac{M}{2\pi RT(x,t)}}\left(S_g+S_b+\frac{\gamma M}{RT(x,t)\rho_0}(S_gK_g+S_bK_b)\right) - P_{gas}(T(x,t))\alpha\sqrt{\frac{M}{2\pi RT(x,t)}}(S_g+S_b)\\
&= \alpha\sqrt{\frac{M}{2\pi RT(x,t)}}\left(P_0e^{-\frac{Q_{sub}}{RT(x,t)}}\left(S_g+S_b+\frac{\gamma M}{RT(x,t)\rho_0}(S_gK_g+S_bK_b)\right) - \frac{(1-\phi)m_{gas}(t)RT(x,t)}{MV_g\phi}(S_g+S_b)\right),
\end{aligned}$$

which is solved by:

$$m_{gas}(x,t) = P_0 e^{-\frac{Q_{sub}}{RT(x,t)}} \left(S_g + S_b + \frac{\gamma M}{RT(x,t)\rho_0}(S_g K_g + S_b K_b) \right) \frac{MV_g\phi}{(1-\phi)RT(x,t)(S_g+S_b)}.$$

Finally, we need to solve for every $x \in \Omega_h$ the system of ODEs given by

$$\frac{\partial}{\partial t}\begin{pmatrix} m_g(x,t) \\ m_b(x,t) \end{pmatrix} = \begin{pmatrix} -J_g\left(t, T(x,t), r_g(x,t), m_{gas}(x,t)\right) S_g(t, r_g(x,t)) \\ -J_b(t, T(x,t), r_b(x,t), m_{gas}(x,t)) S_b(t, r_g(x,t), r_b(x,t)) \end{pmatrix} =: F(f(m_{gb}(x,t)), T(x,t)),$$

where $m_{gb}(x,t) := (m_g(x,t), m_b(x,t))^T$. Because the recovery of the radii via (1.5) needs to be numerically solved, we need to choose the step size τ of a numerical scheme to solve the ODE smaller than the time needed to significantly change the grains/bonds volumes $\tau_{sint_v}(r_b) := \min\{t \geq 0 \mid |V_b(t) - V_b(0)| > \delta, \delta > 0\}$. Mathematically this just means that this system is stiff. In [2] a explicit Euler scheme was used. As this restricts the step size significantly, here in this report we avoid dealing with this issue, by solving the ODE using implicit Euler method:

$$m_i(x, t+\tau) = m_i(x,t) - \tau J_i(x, t+\tau) S_i(x, t+\tau), \quad i = g, b.$$

This is a non-linear root finding problem.

3 Numerical Solution of the PDE

In the Section above we defined the ODE

$$\frac{\partial}{\partial t} m_{gb}(x,t) =: F(f(m_{gb}(x,t)), T(x,t)),$$

where $f(m_{gb}(x,t)) = (r_g(x,t), r_b(x,t))$ and $T(x,t)$ denotes the temperature.
To numerically solve the PDE (1.6) coupled with the ODE we first discretize the state space by $\Omega_h \subset \Omega$ and use the method of lines approach. We integrate both sides from $[x_{i-\frac{1}{2}}, x_{i+\frac{1}{2}}]$ and divide by the length of the interval h:

$$\begin{aligned}
&\rho c_p \frac{\partial}{\partial t} T(x,t) = \frac{\partial}{\partial x} k(x,t) \frac{\partial}{\partial x} T(x,t) \\
&\iff \frac{1}{h}\int_{x_{i-\frac{1}{2}}}^{x_{i+\frac{1}{2}}} \rho c_p \frac{\partial}{\partial t} T(x,t) dx = \frac{1}{h}\int_{x_{i-\frac{1}{2}}}^{x_{i+\frac{1}{2}}} \frac{\partial}{\partial x} k(x,t) \frac{\partial}{\partial x} T(x,t) dx \\
&\iff \frac{1}{h}\int_{x_{i-\frac{1}{2}}}^{x_{i+\frac{1}{2}}} \rho c_p \frac{\partial}{\partial t} T(x,t) dx = \frac{1}{h}\left(k(x_{i+\frac{1}{2}}, t) \frac{\partial}{\partial x} T(x_{i+\frac{1}{2}}, t) - k(x_{i-\frac{1}{2}}, t) \frac{\partial}{\partial x} T(x_{i-\frac{1}{2}}, t) + \mathcal{O}(h^2) \right) \\
&\iff \frac{\partial}{\partial t} \frac{1}{h} \int_{x_{i-\frac{1}{2}}}^{x_{i+\frac{1}{2}}} \rho c_p T(x,t) dx \\
&\quad = \frac{1}{h}\left(k(x_{i+\frac{1}{2}}, t) \frac{T(x_{i+1}, t) - T(x_i, t)}{h} - k(x_{i-\frac{1}{2}}, t) \frac{T(x_i, t) - T(x_{i-1}, t)}{h} + \mathcal{O}(h^2) \right).
\end{aligned}$$

Thus, for every x_i we get the approximate ODE (second order error)

$$\frac{\partial}{\partial t} \frac{1}{h} \int_{x_{i-\frac{1}{2}}}^{x_{i+\frac{1}{2}}} \rho c_p T(x,t) dx \approx k(x_{i+\frac{1}{2}}, t) \frac{T(x_{i+1}, t) - T(x_i, t)}{h^2} - k(x_{i-\frac{1}{2}}, t) \frac{T(x_i, t) - T(x_{i-1}, t)}{h^2}.$$

We will approximate the left hand side integral by its center point (mean value theorem) and thus get the three point method

$$\frac{\partial}{\partial t}\frac{1}{h}\rho c_p T(x_i,t)h \approx k(x_{i+\frac{1}{2}},t)\frac{T(x_{i+1},t)-T(x_i,t)}{h^2} - k(x_{i-\frac{1}{2}},t)\frac{T(x_i,t)-T(x_{i-1},t)}{h^2}.$$

This approximation only holds for the interior of our domain Ω. In order to include the boundary data into the solution we need to handle the Neumann boundary data (1.7) on both sides. This is done by introducing ghost cells. We approximate the boundary data by symmetric differences, i.e. also second order, and get

$$\begin{aligned} k(x_0,t)\frac{T(x_1,t)-T(x_{-1},t)}{2h} + \mathcal{O}(h^2) &= -F_{solar}(t) + \epsilon\sigma_{SB}T(x_0,t)^4 \\ k(x_d,t)\frac{T(x_{d+1},t)-T(x_{d-1},t)}{2h} + \mathcal{O}(h^2) &= 0. \end{aligned}$$

Approximately it holds

$$\begin{aligned} T(x_{-1},t) &\approx \frac{2h}{k(x_0,t)}\left(F_{solar}(t) - \epsilon\sigma_{SB}T(x_0,t)^4\right) + T(x_1,t) =: T_{-1}(t) \\ T(x_{d+1},t) &= T(x_{d-1},t). \end{aligned}$$

In total the following system of ODEs needs to be solved

$$\frac{\partial}{\partial t}\begin{pmatrix} m_{gb}(x_0,t) \\ \rho c_p T(x_0,t) \\ m_{gb}(x_1,t) \\ \rho c_p T(x_1,t) \\ \vdots \\ m_{gb}(x_{d-1},t) \\ \rho c_p T(x_{d-1},t) \\ m_{gb}(x_d,t) \\ \rho c_p T(x_d,t) \end{pmatrix} = \begin{pmatrix} F(f(m_{gb}(x_0,t)),T(x_0,t)) \\ k(x_{\frac{1}{2}},t)\frac{T(x_1,t)-T(x_0,t)}{h^2} - k(x_{-\frac{1}{2}},t)\frac{T(x_0,t)-T_{-1}(t)}{h^2} \\ F(f(m_{gb}(x_1,t)),T(x_1,t)) \\ k(x_{1+\frac{1}{2}},t)\frac{T(x_2,t)-T(x_1,t)}{h^2} - k(x_{1-\frac{1}{2}},t)\frac{T(x_1,t)-T(x_0,t)}{h^2} \\ \vdots \\ F(f(m_{gb}(x_{d-1},t)),T(x_{d-1},t)) \\ k(x_{d-\frac{1}{2}},t)\frac{T(x_d,t)-T(x_{d-1},t)}{h^2} - k(x_{d-\frac{3}{2}},t)\frac{T(x_{d-1},t)-T(x_{d-2},t)}{h^2} \\ F(f(m_{gb}(x_d,t)),T(x_d,t)) \\ k(x_{d+\frac{1}{2}},t)\frac{T(x_{d-1},t)-T(x_d,t)}{h^2} - k(x_{d-\frac{1}{2}},t)\frac{T(x_d,t)-T(x_{d-1},t)}{h^2} \end{pmatrix}$$

which is equivalent to

$$\frac{\partial}{\partial t}\begin{pmatrix} m_{gb}(x_0,t) \\ T(x_0,t) \\ m_{gb}(x_1,t) \\ T(x_1,t) \\ \vdots \\ m_{gb}(x_{d-1},t) \\ T(x_{d-1},t) \\ m_{gb}(x_d,t) \\ T(x_d,t) \end{pmatrix} = \begin{pmatrix} F(f(m_{gb}(x_0,t)),T(x_0,t)) \\ \frac{1}{\rho c_p}\left(k(x_{\frac{1}{2}},t)\frac{T(x_1,t)-T(x_0,t)}{h^2} - k(x_{-\frac{1}{2}},t)\frac{T(x_0,t)-T_{-1}(t)}{h^2}\right) \\ F(f(m_{gb}(x_1,t)),T(x_1,t)) \\ \frac{1}{\rho c_p}\left(k(x_{1+\frac{1}{2}},t)\frac{T(x_2,t)-T(x_1,t)}{h^2} - k(x_{1-\frac{1}{2}},t)\frac{T(x_1,t)-T(x_0,t)}{h^2}\right) \\ \vdots \\ F(f(m_{gb}(x_{d-1},t)),T(x_{d-1},t)) \\ \frac{1}{\rho c_p}\left(k(x_{d-\frac{1}{2}},t)\frac{T(x_d,t)-T(x_{d-1},t)}{h^2} - k(x_{d-\frac{3}{2}},t)\frac{T(x_{d-1},t)-T(x_{d-2},t)}{h^2}\right) \\ F(f(m_{gb}(x_d,t)),T(x_d,t)) \\ \frac{1}{\rho c_p}\left(k(x_{d+\frac{1}{2}},t)\frac{T(x_{d-1},t)-T(x_d,t)}{h^2} - k(x_{d-\frac{1}{2}},t)\frac{T(x_d,t)-T(x_{d-1},t)}{h^2}\right) \end{pmatrix}$$

This is a stiff system of ODEs which is why we solve it via implicit Euler. In the paper [2] MultIHeaTS thermal solver was used.

4 Geometry

Here the volumes of the grains and bonds will be determined, as they are essential in the dynamics of the model.

4.1 Grain Volume

The simple analytic solution for the volume of a quarter grain that is cut of by the hyperplane $\hat{x}^*$ is given by

$$v_g(r_g) := \frac{4}{3}\pi r_g^3 - \frac{\pi(r_g - \hat{x}^*)^2}{3}(2r_g + \hat{x}^*), \tag{1.11}$$

where $\hat{x}^*$ is obtained from the root finding problem in Section 5.4. A more general solution via manifold integrals can be found in the Appendix.

4.2 Bond Volume

As seen in Figure 1.2 there is a circle with radius r_p that satisfies

$$(r_g + r_p)^2 = r_g^2 + (r_b + r_p)^2$$

and solving for r_p yields

$$r_p = \frac{r_b^2}{2(r_g - r_b)}.$$

The area of interest is

$$V^{r_b} := \{x \in \mathbb{R}^3 \mid 0 \le x_1 \le r_g - \hat{x}^*, \sqrt{x_2^2 + x_3^2} \le r_b + r_p - \sqrt{r_p^2 - x_1^2}\}.$$

Denote by $r(x_1) := r_b + r_p - \sqrt{r_p^2 - x_1^2}$, then the Volume is given by

$$\begin{aligned}
&\int_{V^{r_b}} d^3x = \int_0^{r_g - \hat{x}^*} \int_{\{\sqrt{x_2^2 + x_3^2} \le r(x_1)\}} d^2(x_2, x_3)dx_1 = \int_0^{r_g - \hat{x}^*} \pi r(x_1)^2 dx_1 \\
&= \int_0^{r_g - \hat{x}^*} \pi(r_b + r_p)^2 dx_1 - 2(r_b + r_p)\underbrace{\pi \int_0^{r_g - \hat{x}^*} \sqrt{r_p^2 - x_1^2}dx_1}_{=:A} + \pi \int_0^{r_g - \hat{x}^*} r_p^2 dx_1 - \pi \int_0^{r_g - \hat{x}^*} x_1^2 dx_1.
\end{aligned}$$

This is then

$$\begin{aligned}
A &= \pi \left[\frac{x_1}{2}\sqrt{r_p^2 - x_1^2} + \frac{r_p^2}{2}\arcsin\left(\frac{x_1}{r_p}\right) \right]_0^{r_g - \hat{x}^*} \\
&= \pi \left(\frac{r_g - \hat{x}^*}{2}\sqrt{r_p^2 - (r_g - \hat{x}^*)^2} + \frac{r_p^2}{2}\arcsin\left(\frac{r_g - \hat{x}^*}{r_p}\right) \right)
\end{aligned}$$

Finally, we have

$$\begin{aligned}
v_b(r_g, r_b) := \int_{V^{r_p}} d^3x &= \pi(r_b + r_p)^2(r_g - \hat{x}^*) - 2(r_b + r_p)\pi \left(\frac{r_g - \hat{x}^*}{2}\sqrt{r_p^2 - (r_g - \hat{x}^*)^2} + \frac{r_p^2}{2}\arcsin\left(\frac{r_g - \hat{x}^*}{r_p}\right) \right) \\
&\quad + \pi r_p^2(r_g - \hat{x}^*) - \frac{\pi}{3}(r_g - \hat{x}^*)^3.
\end{aligned} \tag{1.12}$$

4.3 Surface Area and Curvature

The surface area in this model, is of crucial importance, as it determines the exchange area of water vapor mass. For the grain we could use the complicated approach from the Appendix and calculate

$$S_g(r_g) = r_g^2 \cdot \left(\pi - 2 \int_0^{\arccos(\frac{\hat{x}^*}{r_g})} \sqrt{1 - \left(\frac{\hat{x}^*}{r_g \cos(\theta)} \right)^2} d\theta \right),$$

but this is too complicated. A simple analytic solution from [2] is given by

$$S_g(r_g) = 4\pi r_g^2 - 2\left(4\pi r_g^2 - 2\pi r_g(r_g - \hat{x}^*)\right) = 4\pi r_g \hat{x}^*.$$

The surface area of the bond is given by the volume of the following set, where $r(x_1) := r_b + r_p - \sqrt{r_p^2 - x_1^2}$:

$$S^{r_b} := \{x \in \mathbb{R}^3 \mid 0 \le x_1 \le r_g - \hat{x}^*, \sqrt{x_2^2 + x_3^2} = r(x_1)\}$$

which is

$$S_b(r_g, r_b) := \int_{S^{r_b}} d\sigma(z) = \int_0^{2\pi} \int_0^{r_g - \hat{x}^*} \sqrt{\det((D\Phi(x,\theta))^T D\Phi(x,\theta))} dx d\theta$$

where $\Phi : [0, r_g - \hat{x}^*] \times [0, 2\pi) \to \mathbb{R}^3, (x, \theta) \mapsto (x, r(x)\cos(\theta), r(x)\sin(\theta))$. Then we get the Jacobian

$$D\Phi = \begin{pmatrix} 1 & 0 \\ r'(x)\cos(\theta) & -r(x)\sin(\theta) \\ r'(x)\sin(\theta) & r(x)\cos(\theta) \end{pmatrix}$$

and thus

$$\begin{aligned} S_b(r_g, r_b) &= \int_0^{2\pi} \int_0^{r_g - \hat{x}^*} r(x)\sqrt{1 + r'(x)^2} dx d\theta \\ &= 2\pi \int_0^{r_g - \hat{x}^*} r(x) \sqrt{1 + \frac{x^2}{r_p^2 - x^2}} dx = 2\pi r_p \left((r_b + r_p)\arcsin(\frac{r_g - \hat{x}^*}{r_p}) - (r_g - \hat{x}^*) \right). \end{aligned}$$

The curvature of the grain is $K_g = \frac{2}{r_g}$ and of the bond $K_b = \frac{1}{r_b} - \frac{1}{r_p}$ respectively. The difference of sign is due to the fact that the bond is concave while the grain is convex.

4.4 Finding the Intersection of Bond and Grain Area

In each time step, the geometry updates, which means that $\hat{x}^*$ changes in every time step, recalling that $\hat{x}^*$ is where the surfaces of the bond and grain intersect. It is the solution of the equation

$$\sqrt{r_g^2 - x^2} = r_b + r_p - \sqrt{r_p^2 - (r_g - x)^2}, \quad x \in (0, r_g). \tag{1.13}$$

This equation for a 4^{th} root of polynomials can be numerically solved and its solution in $(0, r_g)$ gives us $\hat{x}^*$, hopefully uniquely.

2

IMPLEMENTATION

1 Simulations

In this section the results from two different simulations will be presented. In the first we simply assume constant temperature and only consider the sintering process for an individual ice grain and bond. It considers the development of the relative bond grain radius over time for different initial grain radii. In all cases, the original experiment by [1] and the simulation in [2] obtain comparable results as seen in Figure 2.1a. Also the presented simulation, using implicit Euler, gives similar curves as seen in Figure 2.1b.

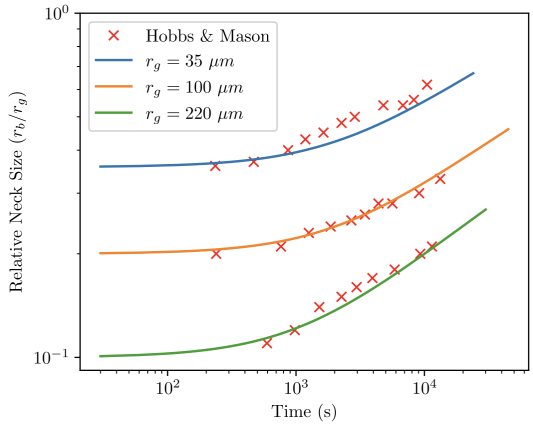

(a) These are the results from [2]. The crosses are data points from [1] and the lines from the model of [2]. They chose constant temperature $-3°C$, sticking coefficient $\alpha = 0.03$ and porosity $\phi = 0.4$.

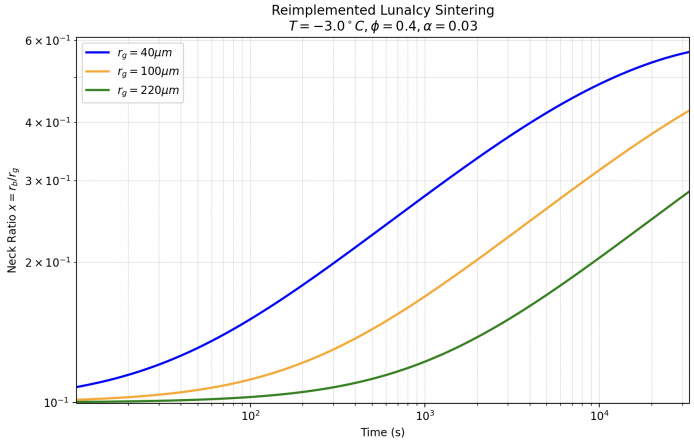

(b) My simulation was carried out with constant temperature $-3°C$, sticking coefficient $\alpha = 0.03$ and porosity $\phi = 0.4$, although the last constant was not mentioned in the caption of Figure 3. in [2].

Figure 2.1

The second simulation considers the entire coupled system, i.e. sintering in every state of the slice of the ice sheet with dynamic temperature described by the PDE. The initial bond radius is set to $r_b = 10^{-5}$ and the initial grain radius to $r_g = 10^{-4}$. Due to computational resource limits, the simulation is run for 10 days only compared to the 1 million years in [2]. Underneath the diurnal skin depth there is no variation in the bond radii, as this is hard coded in the lower boundary condition of the PDE.

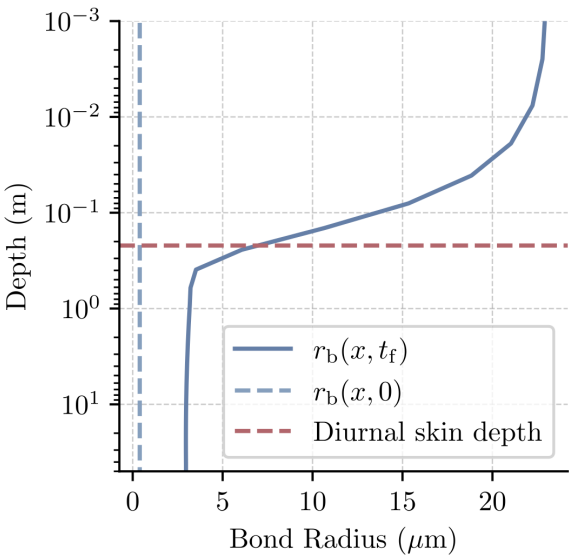

(a) These are the results from [2]. The Bond radius for every depths is plotted after 1 million years of sintering with albedo $A = 0.4$ and porosity of $\phi = 0.8$. The initial bond radius is $r_b(x, 0) \approx 410^{-5}$.

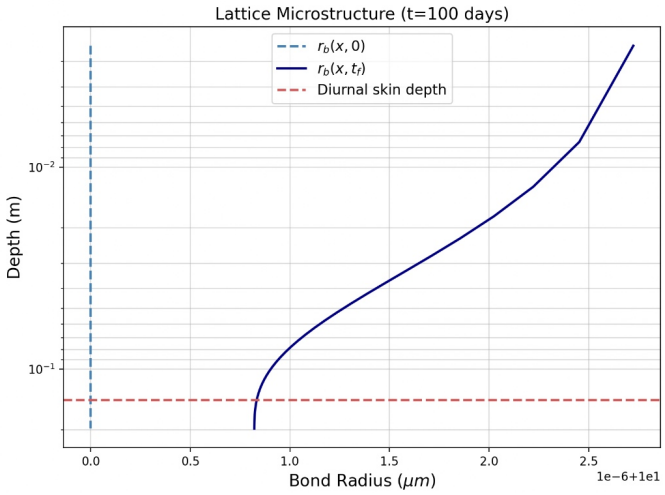

(b) Compared to [2] whose $t_f = 1$ Million years, we get similar results, although here we let it run significantly shorter, $t_f = 100$ Days. The bond radii have increased in size over time. Note that the effect of increasing bond radii is stronger the lower the depth of the grain above the Diurnal skin depth.

Figure 2.2

2 Outlook

This report reimplimented that in a deterministic setting sintering occurs above the diurnal skin depth of Europa's ice sheet. However, as suggested in the intern advertisement, in order to make more realistic predictions on the ice sheet evolution, micro meteor impacts need to be considered. We assume that micro meteorites impacts change the porosity, density of the ice, temperature and mass of gas, grain and bonds. This is why we may consider the larger state vector

$$u(x,t) := (T(x,t), m_g(x,t), m_b(x,t), \phi(x,t), \rho(x,t))^T,$$

where $\phi(x,t)$ is the porosity and $\rho(x,t)$ the density of the ice. Then, including micro meteor impacts, the full stochastic PDE/ODE system is

$$\begin{aligned}
dT(x,t) &= \frac{1}{\rho c_p}\frac{\partial}{\partial x}k(x,t)\frac{\partial}{\partial x}T(x,t)dt + dI^1_{impacts}(x,t)\\
dm_{gb}(x,t) &= F(f(m_{gb}(x,t)), T(x,t))dt + dI^2_{impacts}(x,t)\\
d\phi(x,t) &= G(m_{gb}(x,t), \phi(x,t), T(x,t))dt + dI^3_{impacts}(x,t)\\
d\rho(x,t) &= H(m_{gb}(x,t), \rho(x,t), T(x,t))dt + dI^4_{impacts}(x,t)
\end{aligned}$$

where

$$dI^i_{impacts}(x,t) := \int_{\mathcal{E}} \mathcal{G}_i(\lim_{\epsilon \searrow 0} u(x, t-\epsilon), E)\Phi(dt, dE), \quad i = 1,2,3,4,$$

where Φ is a Poisson point process on $\mathbb{R}^+ \times \mathcal{E}$ with intensity measure $\lambda \times \nu$, where λ is the Lebesgue measure and ν a suitable measure on the space of Energy $\mathcal{E}$ released by the meteor. The functions $\mathcal{G}_i$ describes the

change in the state vector due to an impact of a meteor with energy $E \in \mathcal{E}$. Due to the fact that an impact is assumed to be instantaneously, the resulting stochastic process $u(x,t)_{t\geq 0}$ is a jump process, i.e. càdlàg, which forces us to use left limits in time. As long as there are no impacts, the stochastic integral is zero and the system behaves deterministically. The stochastic integral here over a jump process may be tedious and the theory behind, can be quite complicated. One my attempt to approximate the discontinuities by a stochastic process that is path wise a.s. continuous.
Notably, Φ is a marked Poisson point process, where the marks are energies at each impact of the meteor. As density on the Energy space $\mathcal{E}$ one may use

$$\nu(dE) := A_{surf}\Psi(E)dE, \quad \Psi(E) \sim const.E^{-\beta}.$$

Then the random variable

$$M_T := \sup\{E \in \mathcal{E} \mid (t,E) \in supp(\Phi) \cap [0,T] \times \mathcal{E}\}$$

satisfies by definition of the Poisson distribution

$$\begin{aligned}\mathbb{P}(M_t \leq e) &= \mathbb{P}(\Phi([0,T]\times[e,\infty]) = 0) = \exp(-\lambda(0,T)\cdot\nu([e,\infty])) = \exp(-TA_{surf}\int_e^\infty \Psi(E)dE) \\ &= \exp\left(-TA_{surf}\frac{const.}{\beta-1}e^{-(\beta-1)}\right),\end{aligned}$$

which is a Frèchet distribution. In order to assess worst case scenario impacts, extreme value theory might be taken into consideration.

A

APPENDIX

1 Grain Volume

We begin by calculating 1/4 of the grains volume, where it is cut of at $\hat{x}^*$ at the x_1 axis. This is the volume of the following set:

$$V^{r_g} := \{x \in \mathbb{R}^3 \mid |x| < r_g, 0 \leq x_1 < \hat{x}^*, 0 \leq x_2\}.$$

Further, for $u : \mathbb{R}^3 \to \mathbb{R}, x \mapsto \sqrt{x_1^2 + x_2^2 + x_3^2} = |x|$ the level set u^{-1} describes the set of all points on the sphere S_r^2 with radius r. Clearly, for all $x \in u^{-1}(r)$ the gradient is $\nabla u = \left(\frac{x_1}{r}, \frac{x_2}{r}, \frac{x_3}{r}\right)$ satisfies $|\nabla u| = 1$. With the Co-area formula it holds

$$\int_{V^{r_g}} |\nabla u| d^3x = \int_0^{r_g} \int_{V^{r_g} \cap u^{-1}(r)} d\sigma(z) dr.$$

Define the parametrization $\phi_r : U_r \to V^{r_g} \cap u^{-1}(r), (\theta, \vartheta) \mapsto (r\sin(\vartheta)\cos(\theta), r\sin(\theta)\sin(\vartheta), r\cos(\vartheta))$, where

$$U_r := \{(\theta, \vartheta) \in [0, \frac{\pi}{2}] \times [0, \pi] \mid r\sin(\vartheta)\cos(\theta) < \hat{x}^*\}.$$

Its partial derivatives are

$$\frac{\partial}{\partial\theta}\phi_r(\theta, \vartheta) = (-r\sin(\vartheta)\sin(\theta), r\cos(\theta)\sin(\vartheta), 0)$$
$$\frac{\partial}{\partial\vartheta}\phi_r(\theta, \vartheta) = (r\cos(\vartheta)\cos(\theta), r\sin(\theta)\cos(\vartheta), -r\sin(\vartheta)).$$

Then it holds that

$$\det\left(\begin{pmatrix} (\frac{\partial}{\partial\theta}\phi_r)^T\frac{\partial}{\partial\theta}\phi_r & (\frac{\partial}{\partial\theta}\phi_r)^T\frac{\partial}{\partial\vartheta}\phi_r \\ (\frac{\partial}{\partial\vartheta}\phi_r)^T\frac{\partial}{\partial\theta}\phi_r & (\frac{\partial}{\partial\vartheta}\phi_r)^T\frac{\partial}{\partial\vartheta}\phi_r \end{pmatrix}\right) = \det\left(\begin{pmatrix} r^2\sin(\vartheta)^2 & 0 \\ 0 & r^2 \end{pmatrix}\right) = r^4\sin(\vartheta)^2.$$

Thus, the manifold integral is given by

$$\int_0^{r_g} \int_{V^{r_g} \cap u^{-1}(r)} d\sigma(z) dr = \int_0^{r_g} \int_{U_r} 1 \circ \phi_r(\theta) \sqrt{\det((\phi')^T\phi')} d(\theta, \vartheta) dr$$
$$= \int_0^{r_g} \int_{U_r} 1 \cdot r^2\sin(\vartheta) d(\theta, \vartheta) dr$$

For $\hat{x}^* > r_g$ this integral is trivial equal to $\int_0^{r_g} \pi r^2 dr = \pi\frac{r_g^3}{3}$. More interesting in this application is the opposite case. In order to solve it, we use Fubini (where $U_r^\theta := \{\vartheta \in [0, \pi] \mid (\theta, \vartheta) \in U_r\}$)

$$\int_0^{r_g} \int_{U_r} r^2\sin(\vartheta) d(\theta, \vartheta) dr = \int_0^{r_g} r^2 \int_0^{\pi/2} \int_{U_r^\theta} \sin(\vartheta) d\vartheta d\theta dr$$

We now need to take a closer look at the innermost integral. The condition $\sin(\vartheta) < \frac{\hat{x}^*}{r\cos(\theta)}$ is satisfied if we choose $\theta = arcos(\frac{\hat{x}^*}{r})$ or larger, because

$$\sin(\vartheta) \leq 1 = \frac{\hat{x}^*}{r\cos arcos(\frac{\hat{x}^*}{r})} \text{ is always satisfied.}$$

Thus for $\theta \geq arcos(\frac{\hat{x}^*}{r})$ we need no restriction. For $\theta < arcos(\frac{\hat{x}^*}{r})$ our condition is only satisfied, if

$$\vartheta = \underbrace{arcsin(\frac{\hat{x}^*}{r\cos(\theta)})}_{=:B}$$

or smaller. It is also satified during this choice of $\theta < arcos(\frac{\hat{x}^*}{r})$, if

$$\pi - B < \vartheta \leq \pi, \text{ because } 0 < \sin(\pi - arcsin(\frac{\hat{x}^*}{r\cos(\theta)})) < \frac{\hat{x}^*}{r\cos(arcos(\frac{\hat{x}^*}{r}))} = 1$$

and on that proposed interval $\sin(\vartheta)$ is monotonically decreasing. In total, we get for $r < r_g$:

$$\begin{aligned}
&\int_0^{\pi/2}\int_{U_r^\vartheta}\sin(\vartheta)d\vartheta d\theta = \int_0^{arcos(\frac{\hat{x}^*}{r})}\left(\int_0^B \sin(\vartheta)d\vartheta + \int_{\pi-B}^{\pi}\sin(\vartheta)d\vartheta\right)d\theta + \int_{arcos(\frac{\hat{x}^*}{r})}^{\pi/2}\int_0^{\pi}\sin(\vartheta)d\vartheta d\theta \\
&= \int_0^{arcos(\frac{\hat{x}^*}{r})}\left(\cos(0) - \cos(B) + \cos(\pi - B) - \cos(\pi)\right)d\theta + \int_{arcos(\frac{\hat{x}^*}{r})}^{\pi/2}\cos(0) - \cos(\pi)d\theta \\
&= \int_0^{arcos(\frac{\hat{x}^*}{r})}\left(1 - \cos(B) + \cos(\pi - B) + 1\right)d\theta + \int_{arcos(\frac{\hat{x}^*}{r})}^{\pi/2} 2d\theta \\
&= \int_0^{arcos(\frac{\hat{x}^*}{r})}\left(2 - \cos(B) - \cos(B)\right)d\theta + 2\left(\frac{\pi}{2} - arcos(\frac{\hat{x}^*}{r})\right) \\
&= 2arcos(\frac{\hat{x}^*}{r}) - 2\int_0^{arcos(\frac{\hat{x}^*}{r})}\cos(B)d\theta + \pi - 2arcos(\frac{\hat{x}^*}{r}) \\
&= \pi - 2\int_0^{arcos(\frac{\hat{x}^*}{r})}\cos(arcsin(\frac{\hat{x}^*}{r\cos(\theta)}))d\theta \\
&= \pi - 2\int_0^{arcos(\frac{\hat{x}^*}{r})}\sqrt{1 - \left(\frac{\hat{x}^*}{r\cos(\theta)}\right)^2}d\theta
\end{aligned}$$

Finally for $\hat{x}^* \leq r_g$ we get that

$$\begin{aligned}
&\int_{V^{r_g}} d^3x = \int_0^{r_g} r^2 1_{0\leq r<\hat{x}^*}\left(\pi - 2\cdot 0\right) + r^2\left(\pi - 2\int_0^{arcos(\frac{\hat{x}^*}{r})}\sqrt{1 - \left(\frac{\hat{x}^*}{r\cos(\theta)}\right)^2}d\theta\right)1_{\hat{x}^*<r\leq r_g}dr \\
&= \pi\frac{(\hat{x}^*)^3}{3} + \pi\left(\frac{r_g^3}{3} - \frac{(\hat{x}^*)^3}{3}\right) - 2\int_{\hat{x}^*}^{r_g} r^2 \underbrace{\int_0^{arcos(\frac{\hat{x}^*}{r})}\sqrt{1 - \left(\frac{\hat{x}^*}{r\cos(\theta)}\right)^2}d\theta}_{=:A(\hat{x}^*,r)}dr.
\end{aligned}$$

Note that $A(\hat{x}^*, r)$ does not have an analytical solution and needs to be solved numerically. Note that we only calculated $1/4^{th}$ of its volume, i.e. we need to multiply the resulting value by 4.

BIBLIOGRAPHY

[1] P. V. Hobbs and B. J. Mason. The sintering and adhesion of ice. *Philosophical Magazine*, 9(98):181–197, 1964.

[2] Cyril Mergny and Frédéric Schmidt. Lunaicy: Exploring europa's icy surface microstructure through multiphysics simulations. 2024.